IJMOT

INTERNATIONAL JOURNAL OF MICROWAVE AND OPTICAL TECHNOLOGY,
VOL.13, NO.2, MARCH 2018

Rotational Motion Compensation for Bistatic ISAR Imaging of Non-Uniformly Rotating Targets

Byung-Soo Kang[1]*, Bo-Hyun Ryu[1] Chan-Hong Kim[2], Kyung-Tae Kim[1]

[1] Department of Electrical Engineering, Pohang University of Science and Technology
[2] Agency for Defense Development

E-mail: kkt@postech.ac.kr

***Abstract* – In this paper, we propose a rotational motion compensation (RMC) method for bistatic inverse synthetic aperture radar (Bi-ISAR) imaging. For this, geometry-error, caused by changes of bistatic-angle, is removed using known position information of a transmitter, a receiver, and target trajectories. Next, RMC is conducted to convert non-uniform rotational motion into uniform one. Simulation results using an aircraft model composed of ideal point scatterers validate the efficacy of the proposed Bi-ISAR RMC method.**

***Index Terms* – Bistatic inverse synthetic aperture radar (Bi-ISAR), rotational motion compensation (RMC), non-uniformly rotating target.**

I. INTRODUCTION

Because of many advantages over conventional monostatic inverse synthetic aperture radar (Mo-ISAR) imaging, bistatic ISAR (Bi-ISAR) imaging has attracted much attention in recent years [1–3]. In the past, researches related to Bi-ISAR imaging are subject to condition that rotational motion (RM) of a target is uniform. However, when a target undergoes fast maneuvers, the target can be involved in non-uniform RM. In this case, Bi-ISAR images are significantly blurred unless the non-uniform RM error is properly compensated.

So far, many methods for RM compensation (RMC) have been proposed for Mo-ISAR imaging [4–6]. However, all these methods fail to provide focused Bi-ISAR images of a target in non-uniform RM, because geometry-error is inevitably induced in Bi-ISAR configuration. To address this problem, a new RMC method for Bi-ISAR imaging should be established, but to the best of our knowledge to date, this topic has not yet been sufficiently studied.

In this paper, we propose a new RMC method for Bi-ISAR imaging of non-uniformly rotating target. Unlike conventional RMC process, in the proposed method, bistatic geometry-error is removed using known positon information of a transmitter, a receiver, and trajectories of a target, prior to compensation of non-uniform RM. We should note that correction of the geometry-error enables us to compensate RM error in Bi-ISAR compensation, which is the most remarkable aspect in the proposed method. Consequently, with the proposed method, focused Bi-ISAR images can be formed even when a target undergoes non-uniform RM. Simulation results using an aircraft model composed of ideal point scatterers validate the efficacy of the proposed method.

II. BI-ISAR SIGNAL MODEL

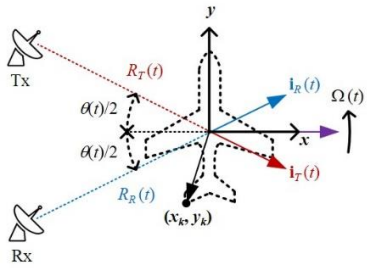


Fig. 1. Geometry for Bi-ISAR imaging.

Fig. 1 shows geometry for Bi-ISAR imaging, where backscattered radar signal in a particular range bin, *n*, can be formulated as [3]:

$$s_n^{BI}(t)=\sum_{k=1}^{L_n}A_k\exp\left\{j\frac{2\pi f_c}{c}\left[R_{BI}(t)+K(t)\left(x_k+y_k\Omega(t)\right)\right]\right\}, \quad (1)$$

where c is the speed of light, f_c is the radar carrier frequency, and $k=1,2,...,L_n$ and L_n are indexes and the total number of scatterers in the *n*th range bin, respectively. $R_{BI}(t)=R_T(t)+R_R(t)$ is translational motion (TM) of the target, $\Omega(t)$ is the RM of the target, and t is slow time. A_k is complex-amplitude of the *k*th scatterer, and (x_k, y_k) are the range and cross-range positions of the *k*th scatterer. In (1), $K(t)$, which carries information about how the bistatic geometry changes with *t*, is defined as:

$$K(t)=2\cos\left[\frac{\theta(t)}{2}\right]\cong K_0+K_1t+K_2t^2, \quad (2)$$

where $\theta(t)$ is the angle between the line of sight (LOS) of a transmitter (Tx) and a receiver (Rx) [i.e., $\mathbf{i}_T(t)$ and $\mathbf{i}_R(t)$ in Fig. 1], which is referred to as bistatic-angle.

We note that any of TM compensation algorithms used in Mo-ISAR configuration can be applicable in Bi-ISAR configuration to remove $R_{BI}(t)$. Following TM compensation, $s_n^{BI}(t)$ in (1) becomes:

$$s_n^{BI}(t)=\sum_{k=1}^{L_n}A_k\exp\left\{j\frac{2\pi f_c}{c}\left[K(t)\left(x_k+y_k\Omega(t)\right)\right]\right\}$$
$$=\sum_{k=1}^{L_n}A_k\exp\left[jh_k^{BI}(t)\right], \quad (3)$$

where

$$h_k^{BI}(t)=\frac{2\pi f_c}{c}\left[K(t)\left(x_k+y_k\Omega(t)\right)\right] \quad (4)$$

is the phase signal of the *k*th scatterer in Bi-ISAR configuration.

In (4), $2\pi f_c K(t)x_k/c$ denotes term of geometry-error, including Bi-ISAR distortion and defocusing. Note that Bi-ISAR distortion yields sheared shape of targets, which makes difficult to use Bi-ISAR images in target classification. Therefore, Bi-ISAR distortion should be restored, which can be efficiently achieved by the methods in [2, 3]. In addition to the Bi-ISAR distortion, geometry-error causes defocusing of Bi-ISAR images, but according to the analysis detailed in [2], this can be neglected in most Bi-ISAR imaging cases.

To obtain focused Bi-ISAR images via Fourier transform (FT) of (3) with respect to t, $\Omega(t)$ should be linearly dependent on t [$\Omega(t)=\omega_1 t$]. However, when a target is in non-uniform RM [$\Omega(t)=\omega_1 t+\omega_2 t^2/2$], Bi-ISAR images are significantly blurred. Unfortunately, the non-uniform RM error cannot be compensated with typical RMC methods [4–6], all of which are used for Mo-ISAR imaging. In the next section, we will describe basis of conventional RMC methods, in which motivations of our work will be presented.

III. MOTIVATION

If Tx and Rx in Fig. 1 are collocated, $\theta(t)=0$ and $K(t)=2\cos\left[\theta(t)/2\right]/2\big|_{\theta(t)=0}=2$. This is equivalent to Mo-ISAR imaging configuration. Then, $s_n^{BI}(t)$ in (2) becomes:

$$s_n^{MO}(t)=\sum_{k=1}^{L_n}A_k\exp\left\{j\frac{2\pi f_c}{c}\left(y_k\Omega(t)\right)\right\}$$
$$=\sum_{k=1}^{L_n}A_k\exp\left[jh_k^{MO}(t)\right], \quad (5)$$

where $h_k^{MO}(t)=2\pi f_c y_k\Omega(t)/2$ is phase signal of the *k*th scatterer in Mo-ISAR configurations. We note that phases of all scatterers in (5) are linearly related to each other, as follows:

$$\frac{1}{y_1}h_1^{MO}(t)=...=\frac{1}{y_k}h_k^{MO}(t)=...=\frac{1}{y_{L_n}}h_{L_n}^{MO}(t). \quad (6)$$

Owing to the linear relationship in (6), all phase signals can be automatically linearized in terms of *t*, if we make one of the phase signals into a linear function of *t*. Namely, relationship in (6) enables us to convert non-uniform RM into uniform one. This is the basis of the existing RMC methods in [4–6].

Unlike (6), phase signals of all scatterers [$h_k^{BI}(t)$] are no longer linearly related to each other in Bi-ISAR configurations. This is due to the term of geometry-error, $2\pi f_c K(t)x_k/c$ in

(4). In this case, if we make one of the phase signals into a linear function of *t*, the phase signals of the remaining scatterers cannot be linearized on *t*. Consequently, typical RMC cannot provide focused Bi-ISAR images owing to the presence of bistatic geometry-error, which motivates us to derive new RMC process for Bi-ISAR imaging.

IV. PROPSED METHOD

In this section, we propose a new RMC process suitable for Bi-ISAR imaging. The first step of the proposed RMC is to correct geometry-error, $2\pi f_c K(t) x_k / c$. In general, modern radar systems can track the movement of a target, and Tx and Rx are usually fixed in a Bi-ISAR configuration. Changes of bistatic angle [$\theta(t)$] can then be obtained using the known position information of the Tx, Rx, and trajectory of the target; $K(t)$ is determined using the relationship in (2). In addition, range positions of scatterers (x_k) are given via known range resolution of $dx = c/[K(0) f_{bw}]$, where f_{bw} is radar bandwidth. Because both $K(t)$ and x_k are known *a priori*, geometry-error, can be corrected as:

$$\begin{aligned}\bar{s}_n^{BI}(t) &= s_n^{BI}(t) g(t) \\ &= \sum_{k=1}^{L_n} A_k \exp\left\{ j \frac{2\pi f_c}{c} \left[K(t) y_k \Omega(t) \right] \right\} \\ &= \sum_{k=1}^{L_n} A_k \exp\left[j \bar{h}_k^{BI}(t) \right],\end{aligned} \quad (7)$$

where $\bar{s}_n^{BI}(t)$ is radar signal after geometry-error correction, and $g(t) = \exp\left[-j2\pi f_c K(t) x_k / c \right]$. It is noteworthy that owing to the geometry-error correction, phases of all scatterers have linear relationship, as follows:

$$\frac{1}{y_1} \bar{h}_1^{BI}(t) = \ldots = \frac{1}{y_k} \bar{h}_k^{BI}(t) = \ldots = \frac{1}{y_{L_n}} \bar{h}_{L_n}^{BI}(t). \quad (8)$$

This enable us to achieve accurate compensation of RM error in Bi-ISAR configuration.

Next, we extract phase signal of a prominent scatterer [$\bar{h}_k^{BI}(t)\big|_{k=l}$] by the methods in [4–6], and define inverse function of $\tau = \left[\bar{h}_l^{BI}(t) \right]^{-1}$ as a new slow variable. Because $\bar{h}_k^{BI}(t) = y_k \bar{h}_l^{BI}(t) / y_l$, and $\bar{h}_l^{BI}(\tau) = t$, phases of all scatterers in (7) become linearly dependent on *t*, when $\bar{s}_n^{BI}(t)$ is reformatted in terms of τ . As a result, focused Bi-ISAR images can be obtained via FT of $\bar{s}_n^{BI}(t)\big|_{t=\tau}$ with respect to τ .

IV. RESULTS

To verify the performance of the proposed method, simulations using an aircraft model, shown in Fig. 2, were conducted. Detailed simulation parameters are listed in Table 1, where the target was involved in non-uniform RM (Fig. 3). Because of the non-uniform RM error, Bi-ISAR images were significantly blurred after TM compensation [3, 7], as shown in Fig. 4(a).

To correct RM error, we performed conventional [6], and the proposed RMC method. It is noteworthy that owing to the presence of geometry error, non-uniform RM cannot be compensated in Bi-ISAR configurations using the conventional RMC method. As a result, Bi-ISAR images are still unfocused even after RMC in [6], as shown in Fig. 4(b). By contrast, with the proposed RMC method, geometry-error is simply corrected using given bistatic-ange [$\theta(t)$]. Therefore, focused Bi-ISAR images were successfully generated, as shown in Fig. 4(c).

Table 1: Simulation parameters for Section IV

.

Carrier frequency	30 GHz
Frequency bandwidth	500 MHz
Number of frequencies per burst	250
Number of bursts	250
Coherent processing interval	3 s
Signal-to-noise ratio	30 dB
Initial bistatic-angle [$\theta(0)$]	$\pi/3$ rad

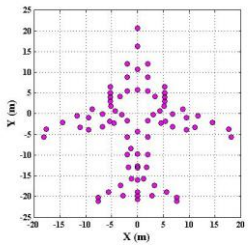


Fig. 2. Aircraft model.

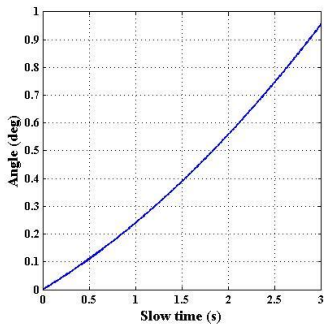


Fig. 3. Non-uniform RM.

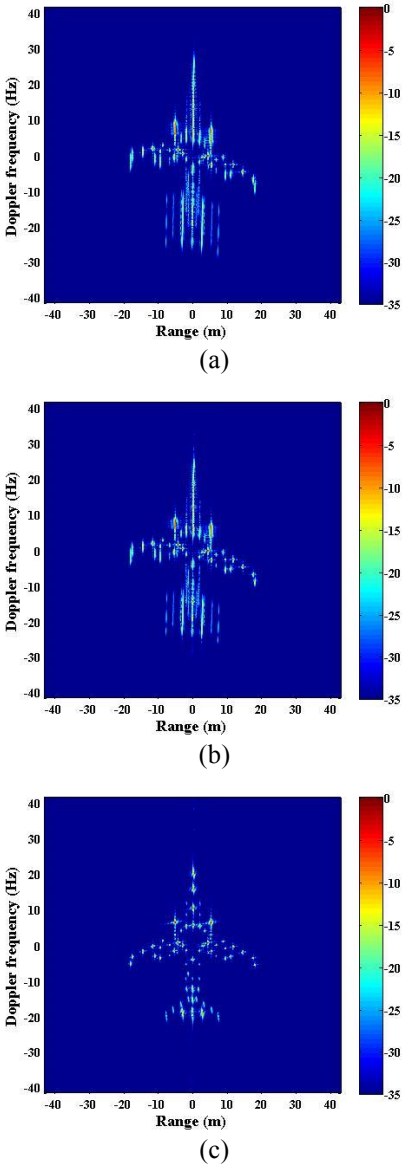


Fig. 4. Bi-ISAR images (a) before RMC, (b) after conventional RMC, and (c) after proposed RMC.

V. CONCLUSIONS

In this paper, RMC method suitable for Bi-ISAR imaging has been proposed. In the proposed method, the geometry-error was corrected by exploiting known position information of Tx, Rx, and target trajectories, followed by TM compensation. Next, new slow variable which converts non-uniform RM into uniform one was found using phase histories of a prominent scatterer. We should note that RM error can be correctly removed with the proposed method, since phase relationship of all scatterers becomes linear, owing to the compensation of geometry-error. As a result, well-focused Bi-ISAR images can be obtained with the proposed method, even when a target exhibits non-uniform RM. In simulations using ideal point scatterers, Bi-ISAR images were significantly blurred when typical RMC was implemented, whereas with our proposed method, well-focused Bi-ISAR images were formed for non-uniformly rotating targets.

ACKNOWLEDGMENT

This work was supported by the Sensor Target Recognition Laboratory (STRL) program of the Defense Development.

REFERENCES

[1] V. C. Chen, and M. Martorella, *Inverse Synthetic Aperture Radar Imaging*, Edison NJ: SciTech, 2014.

[2] Y. Jiang, S. Sun, T. S. Yeo, and Y. Yuan, "Bistatic ISAR distortion and defocusing analysis," *IEEE Trans. Aerosp. Electron. Syst.*, vol. 52, no. 3, pp.1168-1182, Jun. 2016.

[3] B.-S. Kang, J.-H. Bae, M.-S. Kang, E. Yang, and K.-T. Kim, "Bistatic-ISAR cross-range scaling," *IEEE Trans. Aerosp. Electron. Syst.*, accepted for publication.

[4] Y. Wang, H. Ling, and V. C. Chen, "ISAR motion compensation via adaptive joint time-frequency technique," *IEEE Trans. Aerosp. Electron. Syst.*, vol. 34, no. 2, pp. 670-677, Apr. 1998.

[5] W. Brinkman, and T. Thayaparan, "Focusing ISAR images with higher-order motion error using the adaptive joint-time frequency algorithm optimized with genetic algorithm and the particle swarm optimization algorithm-Comparison and results," IET Signal Processing, vol. 4, no. 4, pp. 329-342, Aug. 2010.

[6] B.-S. Kang, J.-H. Bae, S.-J. Lee, C.-H. Kim, and K.-T. Kim, "ISAR rotational motion compensation algorithm using polynomial phase transform," *Microwave and Opt. Tech. Lett.*, vol. 58, no. 7, pp. 1551-1557, Jul. 2016.

[7] J. Wang, and X. Liu, "Improved global range alignment for ISAR," *IEEE Trans. Aerosp. Electron. Syst.*, vol. 43, no. 3, pp.12-17, Jun. 2007.